Bridging the Gap between the Mesoscopic 2D Order-Order Transition and Molecular-Level Reorganization in Dot-Patterned Block Copolymer Monolayers

Marie Richard-Lacroix,[†] Kateryna Borozenko, Christian Pellerin, C. Geraldine Bazuin**

Département de chimie, Centre de recherche sur les matériaux auto–assemblés (CRMAA/CSACS), Université de Montréal, C.P. 6128, succursale Centre-Ville, Montréal (QC), Canada H3C 3J7

KEYWORDS. Block copolymers, Langmuir-Blodgett monolayers, Supramolecular complexes, Order-order transition, Infrared spectroscopy.

ABSTRACT. Langmuir-Blodgett (LB) films of amphiphilic block copolymers (BCs) form well-defined nanostructures with long-range order useful, for instance, for nanolithography applications. Nanostructures with a 2D circular micelle ("dot") morphology are known to present a constant pressure plateau in their Langmuir isotherm (surface pressure vs. molecular area curve at the air/water interface), indicative of a first-order transition. We have previously shown, with LB films of polystyrene-b-poly(4-vinyl pyridine) (PS-P4VP) and its supramolecular complex with 3-n-pentadecylphenol (PDP), that there is an order-order transition of the dots from hexagonal to square at the plateau. However, various literature results indicate that the molecular-level understanding of the transition is poorly understood. Here, using polarized infrared spectroscopy on the PS-P4VP/PDP system, we identify what molecular changes occur at the plateau. The only changes found are an edge-on to isotropic orientation of the pyridine rings and an increase in the level of P4VP hydrogen bonding with PDP; no changes are found in alkyl chain conformation or orientation. Based on these results and AFM observations of the film morphologies, we propose a new mechanism involving 2D to 3D folding of the P4VP chains on the water surface at the plateau pressure that connects the molecular changes with the hexagonal-square reorganization of the dot array. We further show how the model can be generalized to dot-forming LB films of pure PS-P4VP and other BC systems, and even to BC monolayers obtained by spin-coating from dilute solutions. This study thus lays the foundation for a generalized fundamental understanding of dot-forming LB block copolymer films and enables predicting their behavior in order to precisely control their organization and, ultimately, their properties at different length scales.

INTRODUCTION

Block copolymers (BCs) are well known for their ability to phase separate into well-defined nanoscale structures, creating various morphologies driven by parameters such as the affinity between the blocks (χ parameter), their molecular weights and volume ratio, and, in thin films, their interfacial energies with the surrounding media (typically, a substrate and air).[1-3] The Langmuir-Blodgett (LB) technique, with which well-defined structures of molecular-level precision can be fabricated,[4] is useful for producing ultrathin nanostructured films of amphiphilic BCs, most often investigated using diblock copolymers.[5, 6] In this case, the nanostructures are formed at the air/water interface under controlled surface pressure conditions, and the resulting film is then transferred to a solid substrate at constant surface pressure. Typically, the hydrophobic block self-aggregates to minimize its interactions with the water surface and the hydrophilic block spreads as a monolayer to maximize these interactions, leading to 2D surface micellar morphologies such as the so-called dot (or nanodot) and strand (or nanostrand) morphologies where the dots and strands are composed of hydrophobic core aggregates surrounded by a hydrophilic molecular monolayer. These morphologies, or micellar monolayers, can be transferred essentially intact to the solid substrate.

The relative morphological homogeneity and the good long-range order of the structures, whose size, spacing and form depend on the BC composition, molecular weight and block ratio,[7] make LB block copolymer films excellent candidates for forming highly controlled nanoarchitectures for applications, for instance in the area of nanolithography. In recent years, BC templates have attracted attention for their application in non-volatile organic field effect transistors (OFETs),[8-10] where BC complexes act as electronic charge storage electrets[11] leading to high performance non-

volatile memory devices.[12] Chen et al. have also shown a strong correlation of the threshold voltage shifts (*i.e.*, memory window) with inter-micelle distances.[9]

Complexing one of the blocks with small molecules is an efficient way of introducing additional functionality and of tuning both the block volume ratio and the χ parameter to provide access to different morphologies even using a single block copolymer composition.[13-15] This supramolecular strategy has been used extensively in investigations of BC bulk materials[16, 17] and thin films.[13, 18, 19] We investigated LB films of supramolecular complexes of polystyrene-*b*-poly(4-vinyl pyridine) (PS-P4VP) and a phenol-functionalized small molecule, notably 3-*n*-pentadecylphenol (PDP), which hydrogen bonds to P4VP.[7, 20, 21] An important finding using these materials as well as pure PS-P4VP is that LB monolayers with a 2D dot morphology undergo a change in dot order from hexagonal-like at low surface pressure to square-like at higher surface pressure.[21] This morphological transition occurs at a plateau in the Langmuir isotherm (surface pressure as a function of surface area at the air/water interface) that is generally observed for dot-forming BC compositions and that is indicative of a first-order transition.[5, 7, 21] Furthermore, for the PDP-containing system, the order-order transition is accompanied by clear thickening of the PDP/P4VP monolayer matrix.[21]

The high-pressure square pattern is of particular interest since, in general, thin film BC self-assembly of spheres in a 2D plane spontaneously leads to the formation of hexagonal arrays. However, industrial processes for nanopatterning are based on rectilinear systems that require long-range nanoscale square patterns.[22] Complex strategies have been developed to meet these criteria for semiconductor integrated circuit design.[22-25] An additional consideration for some applications is the organization at the molecular scale, particularly the molecular orientation, since it can significantly impact device performance, thus offering a potential route for optimization.

For LB systems with order-order morphological transitions, this orientation may be quite different for transfer pressures below and above the transition pressure.

Despite much investigation, the molecular processes that occur at the plateau and accompany the order-order transition are still controversial. Restricting ourselves to P4VP-based systems, Kawaguchi et al.[26, 27] first deduced from limiting areas of Langmuir isotherms that conformational changes of alkylated P4VP homopolymers (where the P4VP was quaternized by long *n*-alkyl chains) at the air/water interface involve a reorientation of the pyridine rings from flat to edge-on relative to the water surface, with the alkyl chains perpendicular to the surface.[26, 27] It was later proposed, for dot-forming alkylated PS-P4VP diblock copolymers, that the isotherm plateau involves a “starfish” to “jellyfish” transition; i.e. a transition between surface-adsorbed P4VP chains below the plateau to subphase-solubilized P4VP chains above the plateau.[5, 28] This interpretation was subsequently refuted by in situ X-ray and neutron reflectivity experiments, which indicated that the pyridinium layer undergoes significantly less thickening at the plateau than expected from a transition to a "jellyfish" conformation.[29, 30] On the other hand, in situ infrared reflection-absorption spectroscopy indicated greater alkyl chain ordering (greater *trans* conformation) with increasing surface pressure.[29] Based on that observation, we proposed that the above-mentioned thickening of the P4VP/PDP monolayer at the order-order transition was related to PDP reorientation.[21]

In the present contribution, we use polarized infrared (IR) multi-reflection attenuated total reflection (ATR) spectroscopy to directly probe the molecular-level changes that occur at the mesoscopic order-order transition of the dot-forming LB monolayer of PS-P4VP/PDP. Specifically, we investigate possible changes in the alkyl chain conformation, in molecular orientation of various chemical groups, and in hydrogen-bonding interactions in the LB

monolayers transferred at two representative surface pressures, one below and one above the Langmuir isotherm plateau, as representative of hexagonally-ordered and square-ordered dot morphologies, respectively. The analyses lead to the conclusion that the P4VP/PDP monolayer surrounding the dots undergoes a 2D to 3D chain conformational change at the water surface at the order-order transition. Based on these results, we propose a detailed mechanism bridging molecular scale and mesoscale changes associated with the isotherm plateau and show its broad applicability to pure PS-P4VP and other dot-forming BC systems in the literature, and even to spin-coated BC monolayers. This study thus provides a deeper fundamental understanding and, ultimately, will lead to improved control, of the physical properties of nanostructured LB block copolymer films.

EXPERIMENTAL SECTION

Materials. The polystyrene-b-poly(4-vinyl pyridine) (PS-P4VP) block copolymers – one with Mn(PS) = 36,500 g/mol and Mn(P4VP) = 16,000 g/mol (350 S repeat units, 152 VP repeat units, 30.5 mol % P4VP content), referred to hereafter as PS-P4VP(30%), and one with Mn(PS) = 20,000 g/mol and Mn(P4VP) = 17,000 g/mol (192 S repeat units, 162 VP repeat units, 45.9 mol % P4VP content), referred to hereafter as PS-P4VP(46%) – were purchased from Polymer Source (Montreal, Canada) and used as received. 3-n-Pentadecylphenol (PDP, 90%), obtained from Sigma-Aldrich, was recrystallized twice from hexane before use. Chloroform (HPLC grade, EMD Millipore) and anhydrous ethanol (Commercial Alcohols) were used as received. Ultrapure water (18.2 MΩ.cm) was obtained by purification of distilled water with a Millipore Milli-Q Gradient system. Muscovite ruby mica (Hi-Grade, Ted Pella, Redding, USA) was cleaved just prior to immersion into the subphase. The 24-reflection silicon ATR crystal (50 x 20 x 2 mm parallelogram with a 45° face angle; Tydex, St. Petersburg, Russia) was washed successively with chloroform

and ethanol, and then treated with oxygen plasma cleaning (Harrick Plasma Cleaner/Sterilizer PDC-32G) for 5 min just prior to its immersion into the subphase.

Preparation of LB films and Langmuir isotherms. The solutions used for spreading at the air/water interface were prepared by dissolving PS-P4VP in $CHCl_3$ at a concentration of 1.8 mg/mL, to which was added, in the case of PDP-containing solutions, an equimolar amount of PDP relative to the 4VP repeat unit. The solutions were left to stir overnight at room temperature in sealed volumetric flasks. The Langmuir isotherms and LB films were obtained using a computer-controlled Langmuir-Blodgett system (KSV 3000, KSV Instruments, Helsinki, Finland) with a platinum Wilhelmy plate sensing device. The LB trough was first cleaned with $CHCl_3$ and ethanol and then filled with Milli-Q water as the subphase. Its temperature was maintained at 21 ºC using a refrigerated circulator (Isotemp 3016, Fisher Scientific). Before the start of each experiment, a blank compression was performed to verify the cleanliness of the water surface. The block copolymer solution (40 μL) was then spread on the water surface in staggered rows, with the barriers completely open, using a 50-μL Hamilton microliter syringe. After spreading, the solvent ($CHCl_3$) was left to evaporate for 30 min.

Langmuir isotherms of surface pressure (π) as a function of mean molecular area, where molecular area refers to the polymer chain, were obtained by compressing the barriers symmetrically at a constant rate of 10 mm/min (15 cm^2/min). To deposit LB films, the barriers were compressed at the same rate up to the desired surface pressure, which was maintained for 15 min to allow barrier stabilization. The compressed monolayer was then transferred to the solid substrate (submerged in the subphase prior to solution spreading) by vertical withdrawal at a fixed rate of 5 mm/min. The transfer ratio of the deposited PS-P4VP/PDP films was 1.0 ± 0.2, whereas

it was usually lower (0.3-0.5) for pure PS-P4VP. For the latter, the inverse Langmuir-Schaefer technique, which involves horizontal deposition of the monolayer,[21, 31] was also used.

AFM analysis. After deposition on mica substrates, the LB monolayer films were dried in a clean box overnight at room temperature and then scanned by atomic force microscopy (AFM) in tapping mode, using a multimode AFM with a Nanoscope V controller (Digital Instruments/Veeco) with silicon tips (Bruker, TESPA model, rectangular, no aluminum coating on tip and reflective aluminum coating on backside, spring constant 42 N/m, resonance frequency 320 kHz, tip radius 8 nm; or Nanoworld Innovative Technologies, Arrows NCR model, spring constant 42 N/m, oscillation frequency 285 kHz, tip radius less than 10 nm).

Multiple reflection ATR measurements. After deposition on the 24-reflection Si crystal (initial attempts with a 24-reflection Ge crystal led to inconclusive results, which appeared to be related to a low LB transfer ratio, possibly due to poor affinity between the monolayer and the Ge substrate), the LB monolayer films were positioned in a Tensor 27 FT-IR spectrometer (Bruker Optics) equipped with a HgCdTe detector cooled by liquid nitrogen and a vertical ATR accessory, and prepared for analysis by appropriate alignment and purging procedures. The spectra were recorded by averaging 512 scans with 4-cm^{-1} resolution. Single-beam polarized spectra were obtained by successively polarizing the IR beam parallel (p) and perpendicular (s) to the incident plane with a KRS-5 holographic polarizer (Optometrics). Polarized background single beam spectra were then recorded in order to calculate the sample absorbance spectra. This was accomplished by removing the LB film from the crystal using cotton swabs soaked in $CHCl_3$, while being careful not to disturb its position in the sample holder, to avoid spectral distortion.

Orientation quantification. Orientation was quantified using the Harrick thin films approximation, following a procedure described in detail elsewhere.[32] The first coefficient, $\langle P_2 \rangle$,

of the orientation distribution function, which is a series of even Legendre polynomials, can be extracted from IR spectroscopy measurements. In the ATR geometry, the $\langle P_2 \rangle$ values are 0, 1 and -0.5 for a totally isotropic orientation, for perfect orientation along the normal to the substrate, and for perfect orientation in the plane of the substrate, respectively.

The dichroic ratio (R) for a given band must first be quantified from the absorbance recorded with p (A_p) and s (A_s) polarizations as

$$R = \frac{A_p}{A_s} \quad (1)$$

Assuming uniaxial symmetry with respect to the substrate normal (Z axis), the ($\langle P_2 \rangle_{units}$) value, the orientation parameter of the transition dipole moment of a given vibrational mode, can be calculated as

$$\langle P_2 \rangle_{units} = \frac{\langle E_X^2 \rangle - \langle E_Y^2 \rangle R + \langle E_Z^2 \rangle}{\langle E_X^2 \rangle - \langle E_Y^2 \rangle R - 2\langle E_Z^2 \rangle} \quad (2)$$

where the terms $\langle E_X^2 \rangle$, $\langle E_Y^2 \rangle$ and $\langle E_Z^2 \rangle$ represent the mean-square of the electric field amplitude of the evanescent wave along the X, Y and Z axes, respectively. These terms have values of 1.982, 2.189 and 0.542 in our conditions, as calculated from knowledge of the incident angle of the IR beam (45°) and the refractive indices of the ATR crystal (3.4), the thin film sample (estimated to be 1.45) and the adjacent medium (air).[32]

Using the Legendre addition theorem, the orientation parameter of the transition dipole moment can be converted into the order parameter of the molecular axis of interest, $\langle P_2 \rangle$, by taking into account the tilt angle, β, between the transition dipole moment and the molecular axis.

$$\langle P_2 \rangle = \langle P_2 \rangle_{units} \cdot \frac{2}{(3\langle cos^2 \beta \rangle - 1)} \quad (3)$$

RESULTS

Figure 1 shows the Langmuir isotherms for PS-P4VP(30%)/PDP and PS-P4VP(46%), illustrating the plateau (located here at 36 and 6 mN/m, respectively) that is typically found for dot-forming BC monolayers and indicative of a first-order transition.[5, 7, 21] This Figure also shows the AFM images of monolayer films transferred at surface pressures below and above the isotherm plateau (at 25 and 45 mN/m for PS-P4VP/PDP, the two pressures used for IR analyses, and at 3 and 10 mN/m for PS-P4VP), as well as an image of the PS-P4VP/PDP film transferred just above the plateau pressure (38 mN/m). All but one of these images are for LB films, with the exception explained below. These images illustrate the 2D order-order transition of the dot array from hexagonal-like at surface pressures below the plateau to square-like at surface pressures above the plateau.[7,21] In practice, the square-like order often appears more rectangular-like in LB films, as observed in the image in Figure 1 for the PS-P4VP/PDP LB film transferred at 45 mN/m, which has been attributed to slight deformation occurring during LB transfer.[21] An alternative film transfer method, Langmuir-Schaefer (LS) where the monolayer is horizontally deposited on the substrate, minimizes deformation, allowing the square-like order to be more readily observed.[21] An example of such a film is shown in Figure 1 for the PS-P4VP(46%) monolayer transferred above its plateau pressure (in this case, the LS technique was also helpful for obtaining a good morphology image due to the low transfer ratio of LB films). It must be added here that pure PS-P4VP(30%) is at the strand-dot morphological boundary as a function of composition,[7] as indicated by Figure S1 and the associated text in the Supporting Information, and thus cannot show a clear order-order transition.

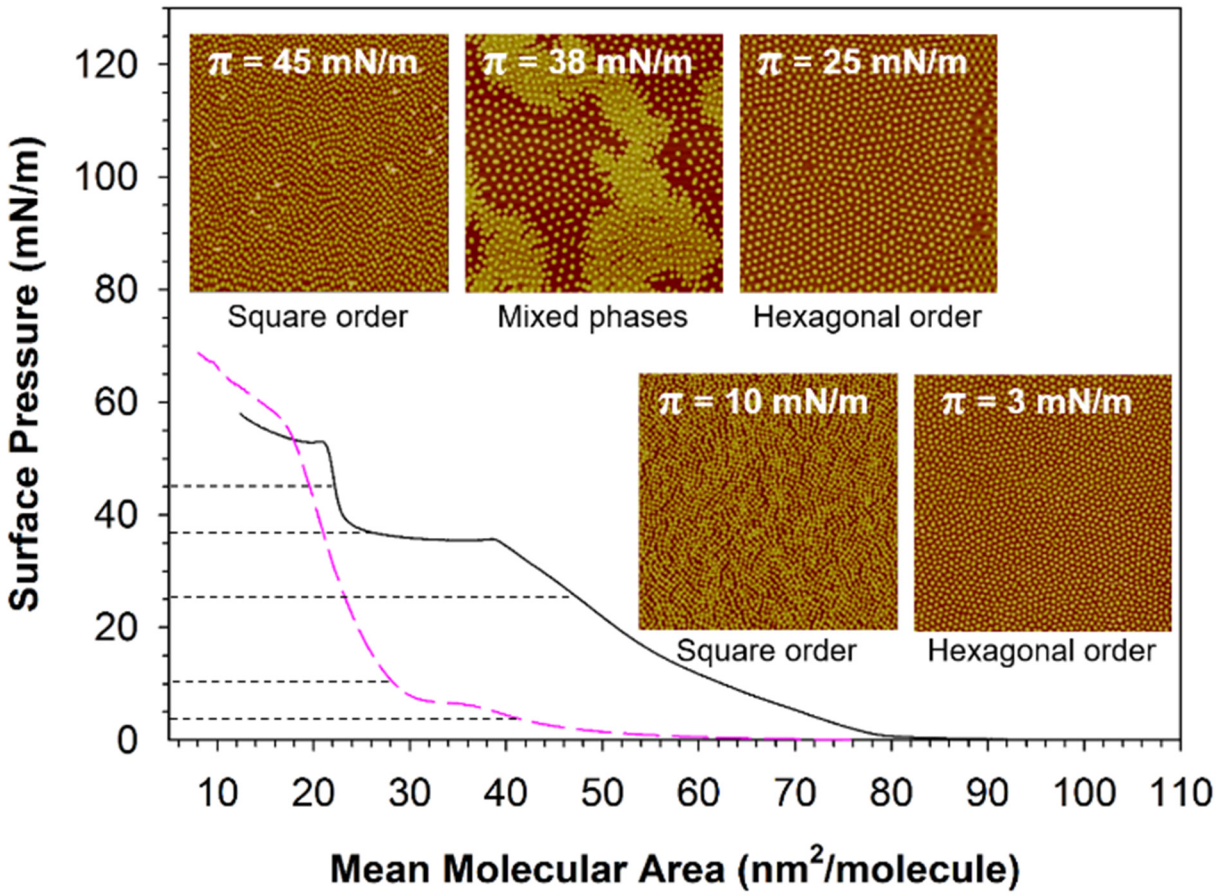

Figure 1. Langmuir compression isotherms of PS-P4VP(30%)/PDP (black) and PS-P4VP(46%) (pink). AFM height images (3x3 μm^2; top three for PS-P4VP/PDP, bottom two for PS-P4VP) of Langmuir-Blodgett monolayer films (Langmuir-Schaefer for PS-P4VP at 10 mN/m) transferred onto mica at the surface pressures indicated on the images and by the dashed horizontal lines.

For the PS-P4VP/PDP LB monolayer transferred at 38 mN/m (in the vicinity of the plateau pressure), the AFM image illustrates a two-phase region where the phases characteristic of the lower and higher pressures are both present.[21] It also clearly shows that the P4VP/PDP matrix, which is on the order of a nm in the low-pressure phase,[21] is significantly thicker in the high-pressure phase, with a difference of 2.8 ± 0.3 nm as measured from AFM height profiles across both phases. The height of the PS dots relative to the low-pressure matrix, about 8 nm for the present system, is similar in the two phases.[21] The similarity of the change in matrix thickness to

the molecular length of PDP, combined with the IR observations by Shin et al.[29] on analogous alkylated PS-P4VP monolayers showing increased *trans* conformation of the alkyl chains at higher surface pressure, previously led to the hypothesis that the PDP molecules undergo an orientational change from essentially prone to essentially vertical (relative to the substrate) at the plateau pressure.[21]

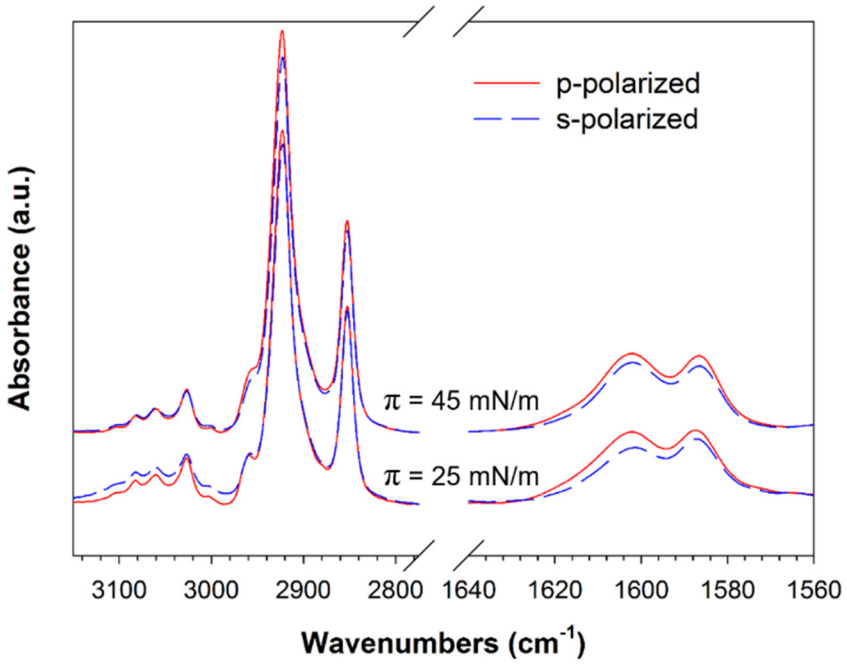

Figure 2. Polarized ATR spectra of Langmuir-Blodgett PS-P4VP(30%)/PDP films transferred to a silicon crystal at the surface pressures indicated.

To better understand what molecular-level changes may occur at the isotherm plateau in the PS-P4VP(30%)/PDP system, we first investigated the alkyl chain conformation of LB films transferred below and above the plateau pressure, as indicated by the polarized ATR spectra in Figure 2. They show that the positions of the symmetric and anti-symmetric CH_2 stretching modes in the 2800-3000 cm^{-1} region are, in fact, identical for both surface pressures. This excludes the possibility that conformational changes of the PDP alkyl chains are associated with the plateau.

Furthermore, the band positions indicate that the alkyl chains are mainly in the disordered *gauche* conformation. The detailed analysis of these bands as well as a comparison with pure PDP in different phases is given in the Supporting Information (see Fig. S2, Table S1 and associated text).

The absence of conformational changes with surface pressure does not exclude the possibility of changes in orientation of the alkyl chains and/or other molecular groups, which was next investigated. Reliable quantification of the molecular orientation (described in the Experimental section) is made possible by the high signal-to-noise ratio of the "s" and "p"-polarized spectra, as shown in Figure 2. Table 1 summarizes the $\langle P_2 \rangle$ values, which are averages of measurements on three independent samples prepared in the same conditions, for various molecular moieties. The standard deviation is very low for all of the bands investigated, highlighting the good reproducibility of the results. The $\langle P_2 \rangle$ values are about 0.3 for the PDP alkyl chains, as determined from the CH_2 stretching bands using a tilt angle of 90° for the transition dipole moment,[33] indicating a relatively high average orientation of the alkyl chains perpendicular to the surface plane (Table 1). Importantly, there is no significant difference below and above the isotherm plateau pressure, at odds with the hypothesis that the change in thickness of the P4VP/PDP matrix at the plateau pressure is due to a reorientation of the PDP chains. Furthermore, for the PDP phenol group, the $\langle P_2 \rangle$ values, measured using the 1586 cm^{-1} band assigned to aromatic C=C stretching, indicate an isotropic distribution both below and above the plateau pressure. This leads to the conclusion that there are no changes in either conformation or orientation for any of the PDP molecular moieties at the plateau pressure.

Next, the orientation of the block copolymer moieties was examined. The orientation of the PS chains composing the dots was determined using the 3060 cm^{-1} band assigned to C-H stretching of the phenyl ring,[34] a band dominated by PS even if P4VP also absorbs in this spectral range (see

Figure S3, Supporting Information). Unsurprisingly, the $\langle P_2 \rangle$ values are close to 0 for both surface pressures, indicating that the PS aromatic rings (and most likely the PS backbone chains as well) are randomly oriented with respect to the surface normal.

Table 1. Orientation Values ($\langle P_2 \rangle$) for the Molecular Moieties of PS-P4VP(30%)/PDP, Obtained from Polarized ATR Spectra of LB Films Transferred to Silicon Substrates at the Surface Pressures (π) Indicated.

Moiety	**Band position (cm^{-1})**	**$\langle P_2 \rangle$ value ***	
		π = 25 mN/m	**π = 45 mN/m**
PS aromatic ring	3060	0.02 ± 0.01	0.00 ± 0.02
PDP alkyl chain	2923	0.32 ± 0.04	0.28 ± 0.06
	2853	0.37 ± 0.05	0.34 ± 0.06
P4VP and PS aromatic rings	1600	0.21 ± 0.03	0.02 ± 0.03
PDP phenol ring	1586	0.01 ± 0.01	0.02 ± 0.01

* Averaged over three independent samples

Interestingly, and in contrast to the results obtained for the PS and PDP moieties, significant changes between low and high transfer pressure are observed in the P4VP pyridine ring orientation, determined using the 1600 cm^{-1} band.[35] DFT calculations indicate that this mode is along the pyridine C1-N axis and thus, perpendicular to the main chain. At low pressure (25 mN/m), the pyridine rings have an average $\langle P_2 \rangle$ value of 0.21, indicative of orientation perpendicular to the substrate plane. Since the 1600 cm^{-1} band includes a minor contribution from the PS aromatic ring stretching (see Figure S4), which is isotropic, the true $\langle P_2 \rangle$ value associated with the pyridine rings must actually be higher than 0.21. At high surface pressure (π=45 mN/m), to our surprise, we found that the $\langle P_2 \rangle$ value is essentially 0, indicating isotropic orientation. This reveals that the molecular

changes associated with the isotherm transition are mainly related to reorganization of the pyridine rings (rather than to alkyl chain reorganization), at least in the present system. It should be added that similar data could not be obtained for the LB films of pure PS-P4VP(46%) due to the weakness of the signal of the polarized spectra, which may be related to the generally low LB transfer ratio for these films (furthermore, analysis of LS films is prevented by the long times necessary to rid the films completely of water, allowing contamination of the film surface by airborne particles).

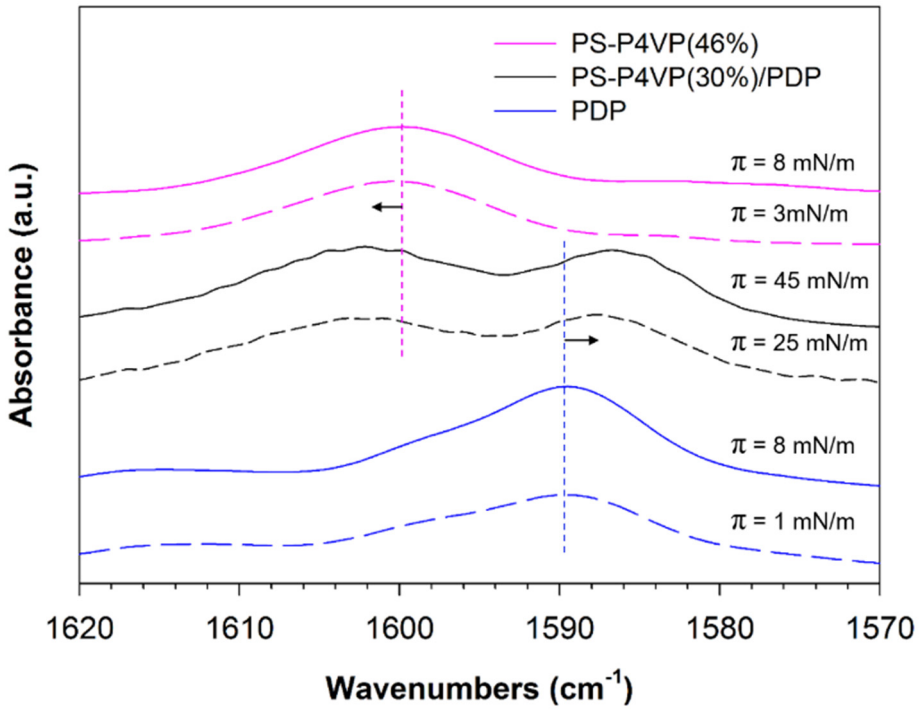

Figure 3. IR spectra in p-polarization for LB films of PDP, PS-P4VP(46%) and PS-P4VP(30%)/PDP transferred on silicon substrates at the surface pressures (π) indicated.

Further insight may be gained by investigating the degree of complexation between P4VP and PDP and any change with surface pressure. This can be probed using the C=C stretching bands of the aromatic rings of P4VP (1600 cm^{-1}) and PDP (1587 cm^{-1}), whose positions are sensitive to hydrogen bonding. Figure 3 compares the p-polarized spectra of the complex transferred below

and above the plateau pressure, of pure PDP transferred at surface pressures of 1 and 8 mN/m (below and above a pseudo-plateau around 6 mN/m[36]), and of pure PS-P4VP(46%) transferred below and above its isotherm plateau. The C=C stretching band of P4VP is located at 1598 cm^{-1} for the PS-P4VP(46%) copolymer in the bulk. It is known to shift to higher frequency when hydrogen bonded,[37] in proportion to the complexation strength.[38] This band shifts to 1600 cm^{-1} in the LB films of PS-P4VP(46%), which can be attributed to pyridine hydrogen bonding interactions with water molecules and/or hydroxides on the silicon surface. There is no noticeable difference between the transfers below and above the plateau pressure. For the LB films of PS-P4VP(30%)/PDP, i.e. in the presence of PDP, the P4VP band further shifts to 1602 cm^{-1}, which can be related to a higher complexation strength with PDP. As shown in Table 2, this shift is again very similar below and above the plateau pressure.

The phenol moiety of the PDP molecules shows quite different behavior, as illustrated in Figure 3. The band for this group is located at ~1589 cm^{-1} for the pure PDP melt (Figure S3) as well as for the pure PDP LB monolayers at both low and high surface pressures, whereas it shifts to ~1587 cm^{-1} in the PS-P4VP(30%)/PDP monolayers (and is also significantly narrower). The similarity for pure PDP in the melt and in LB monolayers can be explained by the similar phenol interactions, notably phenol-phenol for the former and phenol-oxide or phenol-hydroxide (silicon surface and/or water) for the latter, which all involve H-bonding with oxygen acceptors. On the other hand, the shift of the PDP band in the PS-P4VP/PDP monolayers to lower wavenumbers is consistent with the greater interaction strength of the phenol-pyridine hydrogen bond. In contrast to the pyridine ring, for which there is no detectable change in band position between low and high transfer pressures, the PDP phenol band shows a clearly detectable additional shift to lower wavenumbers, from 1587.5 cm^{-1} at low transfer pressure to 1586.8 cm^{-1} at high transfer pressure

(Table 2). This small but reproducible difference can be explained by increased phenol-pyridine interactions in the films transferred at high surface pressure compared to those transferred at low surface pressure. (For further comparison, Figure S4 shows that an even greater shift, to ~1586 cm^{-1}, occurs in the bulk complex due to still greater complexation with pyridine in the bulk than in the monolayers.)

Table 2. Band Positions of the P4VP Pyridine Ring and PDP Phenol Group in PS-P4VP(30%)/PDP Monolayers Transferred at the Surface Pressures (π) Indicated.

	Band position (cm^{-1}) *	
	π = 25 mN/m	**π = 45 mN/m**
P4VP	1602.45 ± 0.02	1602.1 ± 0.1
PDP	1587.48 ± 0.04	1586.79 ± 0.02

* Averaged over three independent samples

DISCUSSION

Molecular-level model of PS-P4VP/PDP LB films below and above the plateau pressure. The main conclusions of the analysis of the IR spectra are summarized in Table 3 and a molecular model that can rationalize these observations is shown in Scheme 1. A common approximation in surface science is to quantify a tilt angle from the $\langle P_2 \rangle$ values. However, it is entropically unlikely that all of the units would be perfectly aligned at this angle, as compared to a smooth unimodal distribution of tilt angles.[39, 40] The molecular orientations indicated in the scheme therefore represent an orientation distribution with a width that is inversely proportional to the $\langle P_2 \rangle$ value.

The random organization of the PS chains in the dot aggregates (orange blobs) and the lack of orientational change upon compression can be related to their glassy state (PS has a high glass

Table 3. Principal Conclusions from IR Spectral Analyses of PS-P4VP/PDP Complexes Transferred to Silicon Substrates at Surface Pressures (π) Below and Above the Isotherm Plateau.

<table>
<tr><th>Unit</th><th>π = 25 mN/m</th><th>π = 45 mN/m</th></tr>
<tr><td rowspan="3">PDP
(blue)</td><td colspan="2">Alkyl chains mainly gauche and oriented perpendicular to substrate; no change with π</td></tr>
<tr><td colspan="2">Isotropic phenol groups</td></tr>
<tr><td>H-bonding to
pyridine present</td><td>H-bonding to
pyridine greater than at low π</td></tr>
<tr><td>PS
(orange)</td><td colspan="2">Isotropic chains</td></tr>
<tr><td rowspan="2">P4VP
(green)</td><td>Pyridine rings oriented perpendicular to substrate</td><td>Isotropic pyridine rings</td></tr>
<tr><td colspan="2">H-bonding strength same at low and high π</td></tr>
</table>

transition temperature and is hardly plasticized by water). In contrast, the position of the (green) P4VP pyridine and (blue) PDP phenol moieties adjacent to the polar surface below the isotherm plateau, as illustrated in Scheme 1 (bottom panel), allows them to interact by H-bonding with the substrate as well as with each other. The interactions with the substrate account for the global out-of-plane orientation of the pyridine rings with respect to the substrate, where the nitrogen atoms must be oriented on average towards the substrate. In contrast, the pyridines become essentially isotropic at high transfer pressures where the matrix thickness was shown by AFM to increase. This loss of surface pinning, represented in Scheme 1 (top panel), allows increased H-bonding interactions of the pyridine groups with the phenol groups of PDP at the expense of pyridine with the substrate. It thereby explains the changes observed in the phenol H-bonding strength that led to the conclusion of greater phenol-pyridine H-bonding above compared to below the plateau

pressure. This change of H-bonding strength is not observed in the pyridine band because the pyridine interactions occur with hydroxyl groups whether on PDP or the substrate (Si or water).

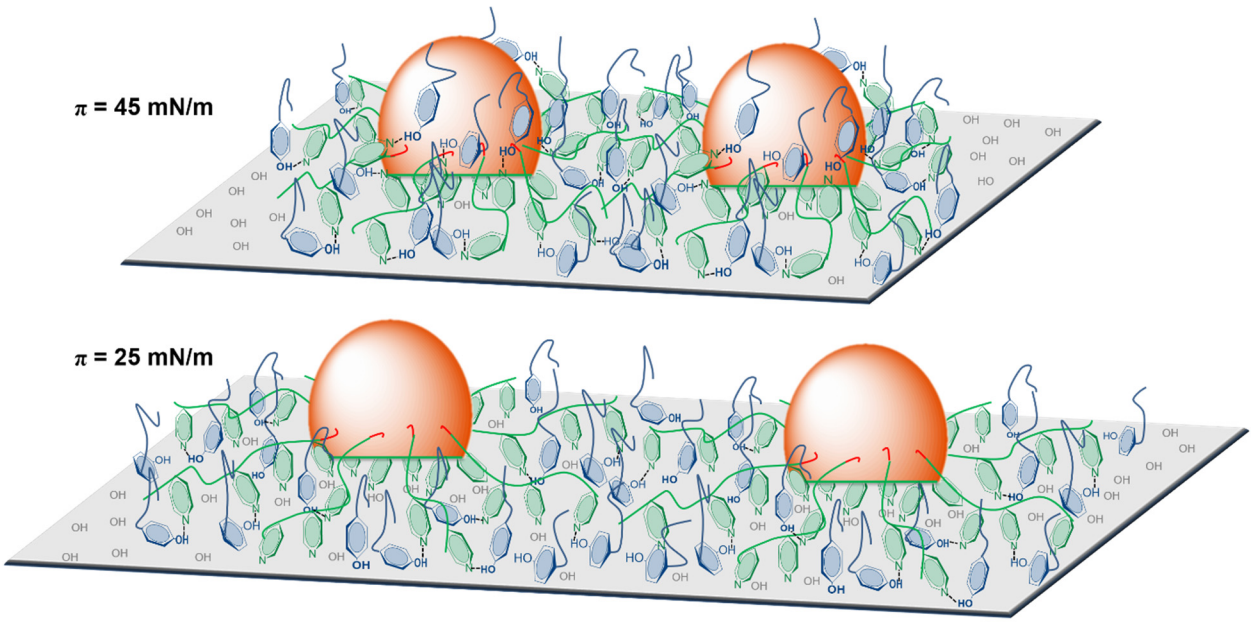

Scheme 1. Model Describing the Molecular Organization of the Dot-Forming PS-P4VP/PDP System Below (Bottom Panel) and Above (Top Panel) the Plateau Pressure in the Langmuir Isotherm. The orange blobs represent the PS aggregates forming a 2D array of dots (with dimensions, not drawn to scale, on the order of 50 nm in diameter, 5-8 nm in relative height, and 80-100 nm in center-to-center distance for the present system, where height and distance are smaller above the plateau than below). P4VP and PDP are shown in green and blue, respectively, and form the LB molecular monolayer matrix. For samples transferred onto silicon substrates at a surface pressure of 25 mN/m (bottom panel), the pyridine rings and alkyl chains show a preferential orientation along the surface normal. The pyridine rings of P4VP and the phenol groups of PDP are complexed either with each other or with the OH groups of the activated silicon substrate. For samples transferred at 45 mN/m (top panel), only the alkyl chains preserve their orientation along the substrate normal; P4VP and PDP are mainly complexed together and the monolayer is partially folded into 3D space, inducing an increase in the matrix thickness.

The PDP alkyl chains maintain overall out-of-plane orientation at both pressures and are located preferentially at the interface with air to minimize surface tension. The absence of conformational change contrasts with the observations by Shin et al. on octadecylated and decylated PS-P4VP monolayers at the air/water interface, who found from in situ IR reflection-absorption analysis that there is increasing *trans* conformation with increase in surface pressure.[29] Whatever the reason for the difference between our system and theirs (some possibilities are discussed in Section D of the Supporting Information), alkyl chain conformational change is clearly not essential to the order-order transition on the molecular level.

Mechanism connecting the molecular-level changes to the mesoscopic hexagonal-square order-order transition. The foregoing results lead us to propose a global mechanism for the transition occurring at the isotherm plateau of dot-forming amphiphilic diblock copolymers, discussed first for the present PS-P4VP/PDP complex. This mechanism, illustrated in Scheme 2, connects the molecular-level changes, analyzed above by IR, with the mesoscopic hexagonal-square dot reorganization, shown by the AFM images in Figure 1 and detailed in ref 21. Its starting point at very low positive surface pressure, where the entire surface is essentially covered with the BC monolayer, is indicated as point 1 in Scheme 2. Here, the dot separation has been found to be about twice the length of the P4VP block in extended conformation for dot-forming PS-P4VP/PDP[7] and alkylated PS-P4VP.[5, 28] This implies that the P4VP chains, which are adsorbed to the water surface to optimize H-bonding interactions, emerge radially from the dots along the surface such that the P4VP density is highest near the interface with PS. This 2D radial "brush-like conformation" of the P4VP chains, where the rigid PS dots act as pinning surfaces,[41-43] is less favorable entropically than a randomly folded 2D "mushroom-like" conformation. However, it is compensated for by the dispersion of the PDP molecules among these chains, allowing H-bonding

to the pyridine groups (in addition to water molecules) and consequent filling in of the empty interchain space. The dot separation by two extended P4VP chains further implies that there is no interpenetration of P4VP from neighboring micelles, which can be attributed to interchain repulsion.[44, 45] Each 2D micelle can thus be approximated as impenetrable discs lying on the water surface, which, in accordance with geometrical arguments about the most efficient way of filling a 2D area, spontaneously organize into a hexagonal pattern,[46] as shown for point 1 in Scheme 2.

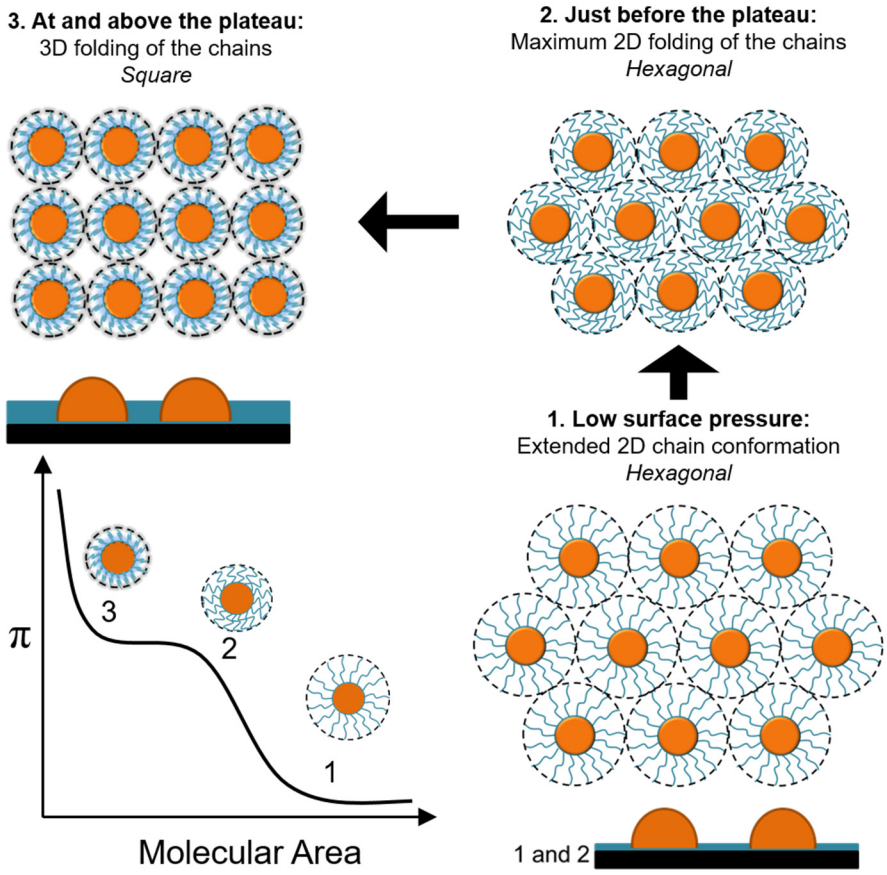

Scheme 2. Schematic Representation of the Chain Conformation and Mesoscopic Organization of the PS-P4VP/PDP Micelles at Different Surface Pressures Along the Langmuir Compression Isotherm. The PS dots are represented as orange blobs and the P4VP/PDP moieties by blue lines. The micelle boundaries are indicated by dashed black circles for simplicity; in reality, the entire space between the PS blobs is expected to be covered with a

P4VP/PDP monolayer. At low surface pressure (point 1 on the Langmuir isotherm), the P4VP chains are in an extended brush-like conformation and the most favorable mesoscopic organization is hexagonal. With increasing surface pressure, the molecular area gradually decreases through 2D folding of the P4VP chains. The plateau begins after maximum 2D chain folding is reached (point 2). At the plateau (point 3), the molecular area decreases due to the 3D chain folding, the matrix thickness increases, and, mesoscopically, the micelles reorganize from hexagonal to square packing.

In increasing the surface pressure to just below the isotherm plateau (point 2 in Scheme 2), the PS dots are pushed closer together, decreasing the dot separation, but their initial size and hexagonal packing order is maintained.[5, 21, 28-30] The invariance in the PS size (based on AFM measurements) implies that the thickness of the P4VP/PDP matrix changes little, if any, from that at point 1, since otherwise the apparent size (height and diameter) should decrease (assuming a hemispherical shape). This is consistent with the IR results for films transferred below the isotherm plateau regarding the average orientation of the pyridine groups towards the surface (water or silicon), which optimizes their contact with the surface like at point 1. These observations can be rationalized by 2D folding of the P4VP chains on the water surface during barrier compression, which both reduces the dot separation with increasing surface pressure and maintains optimal H-bonding interactions with the surface. Maximum 2D chain folding is reached just below the plateau pressure (point 2), where the P4VP conformation can be described as a "compressed 2D brush" throughout which the PDP molecules are dispersed as at point 1. (The term “compressed 2D brush” is used instead of “2D mushroom”, since the chains are still forced by the PDP molecules to be somewhat extended in comparison to the situation for pure PS-P4VP, discussed below.)

At the isotherm plateau pressure, the P4VP chains, having attained their maximal 2D folding, have become incompressible in 2D. At this point, a fraction of the pyridine units sacrifice their

interactions with water and, as depicted for point 3 in Scheme 2, further folding takes place out-of-plane with respect to the water surface, i.e. in 3D space. This leads to the loss of their preferential orientation towards the surface and allows increased complexation with PDP, as indicated by the IR above. This then explains the significant increase in thickness of the P4VP/PDP matrix at the plateau pressure, as described in connection with the AFM image for π = 38 mN/m (Figure 1). It is accompanied by a reduction of the dot diameter,[21] as schematically represented in the lateral views of the films in Scheme 2.

A transition from 2D to 3D P4VP chain folding of P4VP at the air/water interface is consistent with the appearance of a plateau in the Langmuir isotherm, since it implies a large and sudden variation of the molecular area at an essentially constant surface pressure. From a thermodynamic point of view, this feature is well known to be associated with a first-order transition.[47] Its main driving force is entropic, i.e. induced by the significant gain of entropy associated with the freedom of the chains to explore out-of-plane conformations. This entropy gain would compensate for any enthalpic cost of breaking pyridine hydrogen bonds with the surface, which, in any case, is partially offset by additional P4VP-PDP H-bonding.

The association between the 2D-3D changes in chain conformation just described and the simultaneously occurring mesoscopic order-order transition from hexagonal to square can be understood in terms of the increase in dot density under compression made possible by the 3D folding of the P4VP chains. Indeed, simulations of 2D-confined colloidal particles indicated that solid-solid isostructural transitions are promoted by increasing the particle surface density.[46] 2D-confined hard spheres that normally pack hexagonally reorganize under lateral compression, in the simplest scenario, into a square bilayer arrangement.[46, 48, 49] A more refined simulation study of quasi-2D constrained colloidal spheres indicated that the reorganization induces distortions of the

hexagonal lattice, where the particles first begin to undergo in-plane and then out-of-plane motion, leading to the formation of a stable ordered "buckled phase" through a first-order transition that was postulated to be entropically driven.[46, 48] This phase represents an intermediate structure between the hexagonal monolayer and the perfectly square bilayer and is conceptually similar to an imperfectly organized square monolayer phase.[48] These simulations were based on a Marcus-Rice potential designed to represent the features of colloidal particles with grafted polymer brushes to sterically stabilize the system (allowing both repulsive and attractive components in the simulated potentials).[48] The results of these simulations can thus be considered as analogous to the hexagonal-square transition observed here. Accordingly, in the mechanism presented in Scheme 2, the 3D folding of the P4VP chains can be considered to correspond to the simulated "out-of-plane motion" of colloidal particles, enabling the sliding of micelles relative to one another, and the resulting hexagonal-to-square dot reorganization then corresponds to the first-order transition of the colloidal particles from hexagonal to the "imperfect square" (buckled) phase.[46, 48] A more detailed plausible mechanism for this reorganization of the copolymer micelles at the air/water interface, which takes into account probable partial overlap of the P4VP chains (chain interpenetration) in the vicinity of the transition (shown as partial overlapping of the disks), is presented in Figure S4, with commentary, in the Supporting Information.

Generalization of the mechanism to PS-P4VP and other systems. Extension of the above models to other amphiphilic block copolymers will be discussed first for pure PS-P4VP(46%). Its Langmuir isotherm and AFM images are given in Figure 1, showing both an isotherm plateau (at low surface pressure) and the corresponding order-order transition of the dot arrays between hexagonal and square. A detailed comparison of the molecular organization at key surface pressures for PS-P4VP/PDP and pure PS-P4VP is illustrated in Scheme 3. In LB films transferred

at very low surface pressure, the average separation distance between neighboring dots was found to be smaller for pure PS-P4VP than for PS-P4VP/PDP of the same BC composition.[7] Moreover, the shift of the 1600 cm^{-1} pyridine band for pure PS-P4VP LB films compared to the bulk copolymer discussed above indicates strong interactions with the surface. These two facts can be rationalized by the P4VP chains of pure PS-P4VP already being partially folded in an entropically favorable 2D mushroom-like regime at low surface pressure (point 1' in Scheme 3), contrasting with the extended brush conformation caused by the dispersed PDP for the complex (point 1 in Scheme 3).

At points 2 and 2' in Scheme 3, just below their respective plateau pressures, the P4VP chains are compacted maximally in 2D. Since they are already quite folded in mushroom-like conformation at low pressure for pure PS-P4VP, there is much less leeway for additional 2D folding and thus the surface pressure at which maximum 2D folding is reached – i.e. the isotherm plateau pressure – is much lower than is the case for the complex. The surface mobility of the PDP molecules, which is expected to be higher than that of the P4VP chains, may also help in accommodating the 2D folding of the P4VP chains.

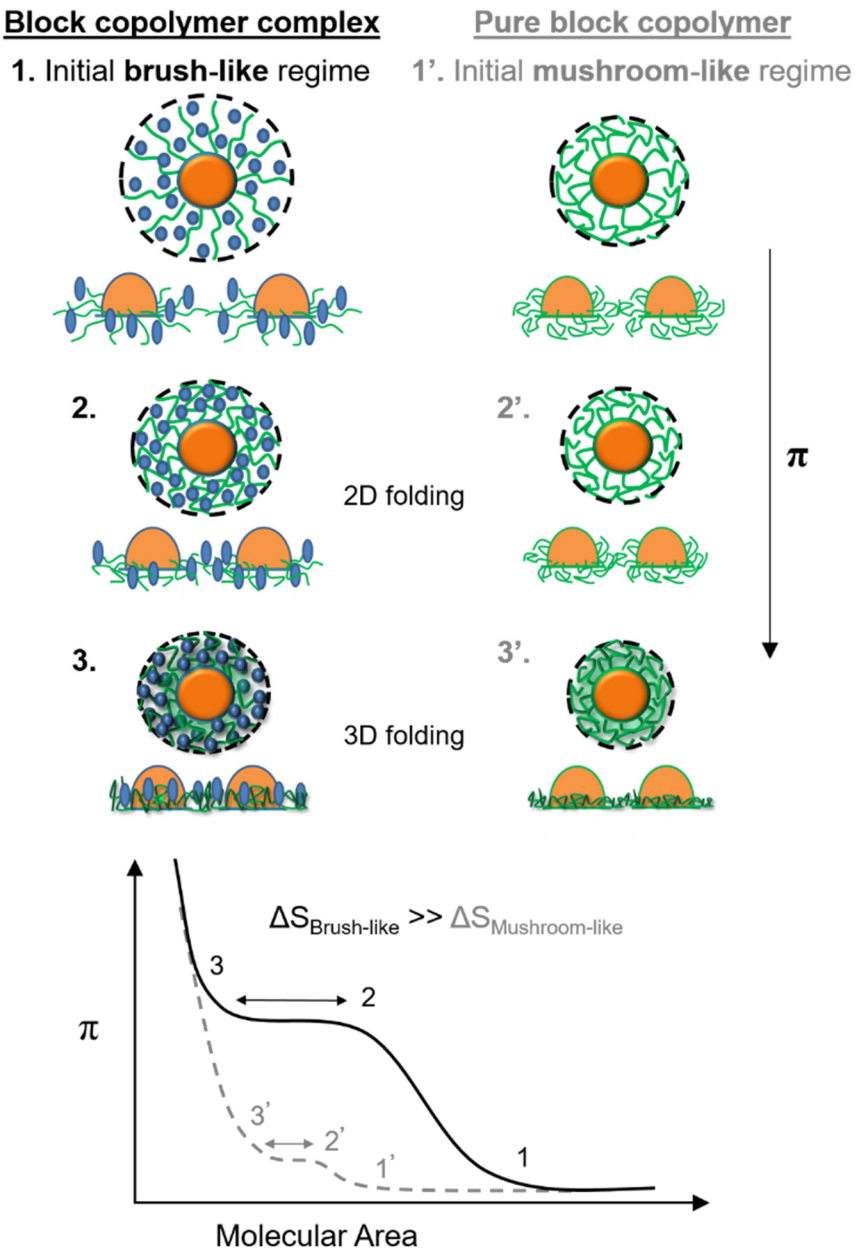

Scheme 3. Model Comparing the Impact of the Presence and Absence of PDP on the Molecular Organization of the P4VP Chains as a Function of Surface Pressure. The hydrophobic PS block in the form of dots, the hydrophilic P4VP chains, and PDP are represented as orange blobs, green chains and blue circles, respectively. Shown are top views of individual micelles and larger lateral views of the system for the three critical points (1-3 for the PDP complex and 1'-3' for the pure BC) indicated on the isotherms (bottom).

Furthermore, the isotherm plateau length – i.e. the reduction in mean molecular area caused by the 3D folding at the transition – is lower for the pure block copolymer compared to the complex (Scheme 3). This can be taken to indicate that the transition at the air/water interface from the 2D compressed mushroom-like regime (point 2') to the 3D mushroom-like regime (point 3') for PS-P4VP involves a smaller molecular area difference than the transition from the 2D compressed brush regime (point 2) to 3D folding (point 3) for PS-P4VP/PDP. From a thermodynamic point of view, the gain in entropy caused by the available third dimension should also be much smaller for the pure BC due to its more favorable initial conformation. The lower compression needed to reach the plateau, the smaller molecular area reduction at the transition and the absence of bulky PDP should all result in a much smaller difference in matrix thickness below and above the plateau for pure PS-P4VP compared to the complex. Indeed, no notable difference in dot height could be detected by AFM in PS-P4VP films transferred below and above the plateau pressure, suggesting that any difference is smaller than the AFM detection limit.

The above mechanism can similarly be applied to interpret observations made on other amphiphilic block copolymer LB films reported in the literature, particularly with regards to the height and length of the isotherm plateau. Regarding the height, Zhu et al. demonstrated that, for dot-forming PS-P4VP with *n*-alkylated pyridine, the plateau surface pressure increases with alkyl chain length (e.g. from 36 mN/m for a C_{10} alkyl chain to more than 55 mN/m for a C_{18} alkyl chain).[50] This is consistent with the proposed mechanism in that the longer the alkyl chain substituent, the larger the area occupied by the alkylated VP repeat unit and the more extended the P4VP backbone (both initially and at the maximum 2D compression); therefore, the larger the entropy gain and area reduction associated at the 2D-3D transition. Similarly, like for pure PS-P4VP, the plateau pressure for dot-forming polystyrene-poly(ethylene oxide) (PS-PEO) (5-10

mN/m) is low, in accordance with the high flexibility of PEO and the small size of the EO repeat unit.[51-54] This also rationalizes the plateau pressures for PS-polydimethylsiloxane (8-10 mN/m), PS-poly(*n*-butyl methacrylate) (10-15 mN/m), and PS-poly(*t*-butyl methacrylate) (15-20 mN/m), noting the somewhat higher values for the latter two due to moderate chain expansion caused by the butyl substituents, which is greater for the bulkier *t*-butyl than for *n*-butyl.[55] In the same vein, the plateau length increases with increase in hydrophilic block content and, especially, block length for dot-forming decylated PS-P4VP,[28] PS-PEO,[52, 53] PS-P4VP/PDP,[7] and PS-P4VP.[7] Again, this is predicted by our model since the entropic gain and the molecular area reduction during the 2D-3D transition should be greater for longer hydrophilic chains.

In addition, the 2D-3D folding mechanism rationalizes the much smaller increase in matrix thickness for alkylated PS-P4VP measured by Shin et al.[29] around the plateau pressure (2-3 nm, similar to what we found for PS-P4VP/PDP) compared to what was to be expected from the starfish-jellyfish model (10-40 nm), leading to its rejection. It should be noted that the starfish-jellyfish model is also a 2D-3D transition, but is distinguished from our model by the fact that the jellyfish state implies a brush-like extension of the hydrophilic block into the subphase perpendicular to the surface as opposed to 3D folding where the hydrophilic chains lie much closer to the water surface. On the other hand, it is not impossible that a jellyfish-like state may be applicable to systems where the hydrophilic block is sufficiently water soluble, as is often considered to be the case for PS-PEO[56] (although one study indicated that PEO homopolymer undergoes combined dehydration and conformational change under pressure at the air/water interface,[28, 57] which is more consistent with 2D-3D folding). This also appeared to be the case for *n*-butylated PS-P4VP when the surface tension of the water subphase was reduced by addition of

1-5 vol % *n*-butanol, for which the matrix thickness was measured to increase by ca. 10 nm at the plateau pressure.[29]

It must be emphasized that the mesoscopic order-order transition of the dot arrays from hexagonal to square (Scheme 2), which we have shown also occurs at the isotherm plateau, appears to be equally general.[21] Not only is it apparent for both PS-P4VP/PDP and pure PS-P4VP (Figure 1), but close inspection of literature data gives hints of such a change in order in images obtained below and above an isotherm plateau, although this was not explicitly reported. These include PS-PEO of MW 250K (see the isotherm in Figure 1a and the AFM images in Figure 2 of ref 52), a PS-poly(methyl methacrylate) sample labeled P155 (see the isotherm of Figure 1, showing a slight plateau, and the AFM images in Figure 2 of ref 58), and even Janus micelles composed of PS-polybutylene-poly(methyl methacrylate) (see the isotherm in Figure 3 and the AFM images in Figure 6b,c in ref 59).

As a final remark, the model may be extended to beyond Langmuir-Blodgett films, given a literature reference where similar behavior can be identified from AFM images of dot-forming PS-P2VP monolayers formed on silicon surfaces by spin-coating.[60] At very low solution concentration, the dot arrays appear hexagonal in order (Figure 3a-i in ref 60), whereas at higher concentration it appears square-like (Figure 2j in ref 60). Although the process of monolayer formation by spin-coating is fundamentally different from LB monolayer formation, a similar mechanism should apply; namely, for low concentrations, the P2VP chains have room to optimize their contact with the substrate in a 2D regime, but they are forced to adopt a 3D conformation, leading to a change of organization of the dots from hexagonal to square, when the surface density is increased by the use of more concentrated solutions.

CONCLUSIONS

We have conducted a detailed polarized infrared investigation of LB films of a dot-forming supramolecular block copolymer system composed of PS-P4VP and PDP, with the aim of identifying what molecular-level changes accompany the mesoscopic order-order transition of the dot array from hexagonal to square associated with a plateau in the Langmuir isotherms of dot-forming BC systems. It was found (a) that the pyridine units of P4VP are oriented perpendicular to the surface at low surface pressures and become isotropic in orientation above the plateau pressure and (b) that there is a greater degree of H-bonding of PDP to P4VP above the plateau pressure than below. No other changes were detected. In particular, the PDP alkyl chains are essentially disordered with a net perpendicular orientation that is the same below and above the plateau.

These results can be rationalized by a mechanism that involves an entropically driven molecular 2D to 3D folding of the P4VP chains on the water surface in association with the mesoscopic order-order transition at the isotherm plateau. This mechanism can be generalized to pure PS-P4VP as well as to other amphiphilic block copolymers showing LB dot morphologies, where the isotherm plateau height reflects the maximum degree of 2D folding that is possible when increasing the surface pressure from near-zero to the plateau and the plateau length reflects the difference in molecular area between maximum 2D folding and initial 3D folding. Thus, for pure PS-P4VP and similar block copolymers, the hydrophilic chains are already partially folded in 2D at near-zero surface pressure, resulting in a plateau at relatively low surface pressure. In contrast, PS-P4VP/PDP and analogous block copolymers with long alkyl chain substituents on the hydrophilic block (e.g. *n*-alkylated P4VP) have highly extended hydrophilic chains at low surface pressure to accommodate the alkyl chains; this allows for extensive 2D chain folding before the maximum folding in 2D is reached , resulting in a plateau at a much higher surface pressure. The

model can be extended to dot-forming BC monolayers prepared by spin-coating. This very fundamental and general understanding of dot-forming monolayer films is important for the intelligent control of their material properties that can impact on the performance of such films in various types of devices.

ASSOCIATED CONTENT

Supporting Information

Complementary information for LB films of PS-P4VP(30 vs. 46%), PDP alkyl chain conformation, IR band positions for PS, P4VP and PDP, and a mechanism for the mesoscopic hexagonal-square transition (PDF). This material is available free of charge via the Internet at http://pubs.acs.org.

AUTHOR INFORMATION

Corresponding Authors

* geraldine.bazuin@umontreal.ca; * c.pellerin@umontreal.ca

Present Address

† Leibniz Institute of Photonic Technology, Albert-Einstein-Strasse 9, 07745 Jena, Germany; Institute of Physical Chemistry and Abbe Center of Photonics, Friedrich-Schiller University Jena, Helmholtzweg 4, 07743 Jena, Germany

Notes

The authors declare no competing financial interest.

ACKNOWLEDGMENTS

The research was supported by grants and a scholarship (MRL) from the Natural Sciences and Engineering Research Council (NSERC) of Canada and the Fonds de Recherche du Québec – Nature et Technologies (FRQ-NT). We thank Prof. Antonella Badia of our department and Dr. Gérald Guérin of the University of Toronto for useful discussions.

REFERENCES

(1) Bates, F. S.; Fredrickson, G. H. Block Copolymer Thermodynamics: Theory and Experiment. *Annu. Rev. Phys. Chem.* **1990,** *41*, 525-557.

(2) Kim, H.-C.; Park, S.-M.; Hinsberg, W. D. Block Copolymer Based Nanostructures: Materials, Processes, and Applications to Electronics. *Chem. Rev.* **2009,** *110*, 146-177.

(3) Segalman, R. A. Patterning with Block Copolymer Thin Films. *Mat. Sci. Eng. R* **2005,** *48*, 191-226.

(4) Ariga, K.; Yamauchi, Y.; Mori, T.; Hill, J. P. 25th Anniversary Article: What Can Be Done with the Langmuir-Blodgett Method? Recent Developments and its Critical Role in Materials Science. *Adv. Mater.* **2013,** *25*, 6477-6512.

(5) Zhu, J.; Eisenberg, A.; Lennox, R. B. Interfacial Behavior of Block Polyelectrolytes. 1. Evidence for Novel Surface Micelle Formation. *J. Am. Chem. Soc.* **1991,** *113*, 5583-5588.

(6) Perepichka, I.; Chen, X.; Bazuin, C. G. Nanopatterning of Substrates by Self-Assembly in Supramolecular Block Copolymer Monolayer Films. *Sci. China Chem.* **2013,** *56*, 48-55.

(7) Perepichka, I. I.; Lu, Q.; Badia, A.; Bazuin, C. G. Understanding and Controlling Morphology Formation in Langmuir–Blodgett Block Copolymer Films Using PS-P4VP and PS-P4VP/PDP. *Langmuir* **2013,** *29*, 4502-4519.

(8) Chi, H.-Y.; Hsu, H.-W.; Tung, S.-H.; Liu, C.-L. Nonvolatile Organic Field-Effect Transistors Memory Devices Using Supramolecular Block Copolymer/Functional Small Molecule Nanocomposite Electret. *ACS Appl. Mater. Interfaces* **2015,** *7*, 5663-5673.

(9) Chen, C.-M.; Liu, C.-M.; Tsai, M.-C.; Chen, H.-C.; Wei, K.-H. A Nanostructured Micellar Diblock Copolymer Layer Affects the Memory Characteristics and Packing of Pentacene Molecules in Non-Volatile Organic Field-Effect Transistor Memory Devices. *J. Mater. Chem. C* **2013,** *1*, 2328-2337.

(10) Cativo, M. H. M.; Kim, D. K.; Riggleman, R. A.; Yager, K. G.; Nonnenmann, S. S.; Chao, H.; Bonnell, D. A.; Black, C. T.; Kagan, C. R.; Park, S.-J. Air–Liquid Interfacial Self-Assembly of Conjugated Block Copolymers into Ordered Nanowire Arrays. *ACS Nano* **2014,** *8*, 12755-12762.

(11) Chou, Y.-H.; Chang, H.-C.; Liu, C.-L.; Chen, W.-C. Polymeric Charge Storage Electrets for Non-Volatile Organic Field Effect Transistor Memory Devices. *Polym. Chem.* **2015,** *6*, 341-352.

(12) Chou, Y. H.; Chiu, Y. C.; Lee, W. Y.; Chen, W. C. Non-Volatile Organic Transistor Memory Devices using the Poly(4-vinylpyridine)-Based Supramolecular Electrets. *Chem. Comm.* **2015,** *51*, 2562-2564.

(13) Nandan, B.; Vyas, M. K.; Böhme, M.; Stamm, M. Composition-Dependent Morphological Transitions and Pathways in Switching of Fine Structure in Thin Films of Block Copolymer Supramolecular Assemblies. *Macromolecules* **2010,** *43*, 2463-2473.

(14) Kuila, B. K.; Chakraborty, C.; Malik, S. A Synergistic Coassembly of Block Copolymer and Fluorescent Probe in Thin Film for Fine-Tuning the Block Copolymer Morphology and Luminescence Property of the Probe Molecules. *Macromolecules* **2013,** *46*, 484-492.

(15) Daga, V. K.; Watkins, J. J. Hydrogen-Bond-Mediated Phase Behavior of Complexes of Small Molecule Additives with Poly(ethylene oxide-b-propylene oxide-b-ethylene oxide) Triblock Copolymer Surfactants. *Macromolecules* **2010,** *43*, 9990-9997.

(16) Ruokolainen, J.; Mäkinen, R.; Torkkeli, M.; Mäkelä, T.; Serimaa, R.; ten Brinke, G.; Ikkala, O. Switching Supramolecular Polymeric Materials with Multiple Length Scales. *Science* **1998,** *280*, 557-560.

(17) Tung, S.-H.; Kalarickal, N. C.; Mays, J. W.; Xu, T. Hierarchical Assemblies of Block-Copolymer-Based Supramolecules in Thin Films. *Macromolecules* **2008,** *41*, 6453-6462.

(18) Roland, S.; Gamys, C. G.; Grosrenaud, J.; Boissé, S.; Pellerin, C.; Prud'homme, R. E.; Bazuin, C. G. Solvent Influence on Thickness, Composition, and Morphology Variation with Dip-Coating Rate in Supramolecular PS-b-P4VP Thin Films. *Macromolecules* **2015,** *48*, 4823-4834.

(19) van Zoelen, W.; ten Brinke, G. Thin Films of Complexed Block Copolymers. *Soft Matter* **2009,** *5*, 1568-1582.

(20) Perepichka, I. I.; Badia, A.; Bazuin, C. G. Nanostrand Formation of Block Copolymers at the Air/Water Interface. *ACS Nano* **2010,** *4*, 6825-6835.

(21) Perepichka, I. I.; Borozenko, K.; Badia, A.; Bazuin, C. G. Pressure-Induced Order Transition in Nanodot-Forming Diblock Copolymers at the Air/Water Interface. *J. Am. Chem. Soc.* **2011,** *133*, 19702-19705.

(22) Tang, C.; Lennon, E. M.; Fredrickson, G. H.; Kramer, E. J.; Hawker, C. J. Evolution of Block Copolymer Lithography to Highly Ordered Square Arrays. *Science* **2008,** *322*, 429-432.

(23) Ji, S.; Wan, L.; Liu, C.-C.; Nealey, P. F. Directed Self-assembly of Block Copolymers on Chemical Patterns: A Platform for Nanofabrication. *Prog. Polym. Sci.* **2016,** *54*, 76-127.

(24) Hardy, C. G.; Tang, C. Advances in Square Arrays through Self-Assembly and Directed Self-Assembly of Block Copolymers. *J. Polym. Sci., Part B: Polym. Phys.* **2013,** *51*, 2-15.

(25) Tang, C.; Sivanandan, K.; Stahl, B. C.; Fredrickson, G. H.; Kramer, E. J.; Hawker, C. J. Multiple Nanoscale Templates by Orthogonal Degradation of a Supramolecular Block Copolymer Lithographic System. *ACS Nano* **2010,** *4*, 285-291.

(26) Kawaguchi, M.; Itoh, S.; Takahashi, A. Liquid-Expanded to Liquid-Condensed Phase Transition in Polyelectrolyte Monolayers on the Aqueous KBr Solution. 2. Temperature Dependence. *Macromolecules* **1987,** *20*, 1056-1060.

(27) Kawaguchi, M.; Itoh, S.; Takahashi, A. Liquid-Expanded to Liquid-Condensed Phase Transition in Polyelectrolyte Monolayers on the Aqueous KBr Solution. 1. Salt Concentration Dependence. *Macromolecules* **1987,** *20*, 1052-1056.

(28) Zhu, J.; Eisenberg, A.; Lennox, R. B. Interfacial Behavior of Block Polyelectrolytes. 5. Effect of Varying Block Lengths on the Properties of Surface Micelles. *Macromolecules* **1992,** *25*, 6547-6555.

(29) Shin, K.; Rafailovich, M. H.; Sokolov, J.; Chang, D. M.; Cox, J. K.; Lennox, R. B.; Eisenberg, A.; Gibaud, A.; Huang, J.; Hsu, S. L.; Satija, S. K. Observation of Surface Ordering of

Alkyl Side Chains in Polystyrene/Polyelectrolytes Diblock Copolymer Langmuir Films. *Langmuir* **2001,** *17*, 4955-4961.

(30) Li, Z.; Zhao, W.; Quinn, J.; Rafailovich, M.; Sokolov, J.; Lennox, R.; Eisenberg, A.; Wu, X.; Kim, M.; Sinha, S. X-ray Reflectivity of Diblock Copolymer Monolayers at the Air/Water Interface. *Langmuir* **1995,** *11*, 4785-4792.

(31) Ding, J.; Doudevski, I.; Warriner, H. E.; Alig, T.; Zasadzinski, J. A.; Waring, A. J.; Sherman, M. A. Nanostructure Changes in Lung Surfactant Monolayers Induced by Interactions between Palmitoyloleoylphosphatidylglycerol and Surfactant Protein B. *Langmuir* **2003,** *19*, 1539-1550.

(32) Picard, F.; Buffeteau, T.; Desbat, B.; Auger, M.; Pézolet, M. Quantitative Orientation Measurements in Thin Lipid Films by Attenuated Total Reflection Infrared Spectroscopy. *Biophys. J.* **1999,** *76*, 539-551.

(33) Allara, D. L.; Swalen, J. D. An Infrared Reflection Spectroscopy Study of Oriented Cadmium Arachidate Monolayer Films on Evaporated Silver. *J. Phys. Chem.* **1982,** *86*, 2700-2704.

(34) Jasse, B.; Koenig, J. L. Fourier Transform Infra-Red Study of Uniaxially-Oriented Isotactic Polystyrene. *Polymer* **1981,** *22*, 1040-1044.

(35) Panov, V. P.; Kazarin, L. A.; Dubrovin, V. I.; Gusev, V. V.; Kirsh, Y. É. Infrared Spectra of Atactic Poly-4-vinylpyridine. *J Appl Spectrosc* **1974,** *21*, 1504-1510.

(36) Lu, Q.; Bazuin, C. G. Solvent-Assisted Formation of Nanostrand Networks from Supramolecular Diblock Copolymer/Surfactant Complexes at the Air/Water Interface. *Nano Lett.* **2005,** *5*, 1309-1314.

(37) Ruokolainen, J.; ten Brinke, G.; Ikkala, O.; Torkkeli, M.; Serimaa, R. Mesomorphic Structures in Flexible Polymer−Surfactant Systems Due to Hydrogen Bonding: Poly(4-vinylpyridine)−Pentadecylphenol. *Macromolecules* **1996,** *29*, 3409-3415.

(38) Roland, S.; Pellerin, C.; Bazuin, C. G.; Prud'homme, R. E. Evolution of Small Molecule Content and Morphology with Dip-Coating Rate in Supramolecular PS–P4VP Thin Films. *Macromolecules* **2012,** *45*, 7964-7972.

(39) Richard-Lacroix, M.; Pellerin, C. Novel Method for Quantifying Molecular Orientation by Polarized Raman Spectroscopy: A Comparative Simulations Study. *Appl. Spectrosc.* **2013,** *67*, 409-19.

(40) Richard-Lacroix, M.; Pellerin, C. Accurate New Method for Molecular Orientation Quantification Using Polarized Raman Spectroscopy. *Macromolecules* **2013,** *46*, 5561-5569.

(41) Wu, T.; Efimenko, K.; Genzer, J. Combinatorial Study of the Mushroom-to-Brush Crossover in Surface Anchored Polyacrylamide. *J. Am. Chem. Soc.* **2002,** *124*, 9394-9395.

(42) Brittain, W. J.; Minko, S. A Structural Definition of Polymer Brushes. *J. Polym. Sci. A: Polym. Chem.* **2007,** *45*, 3505-3512.

(43) de Gennes, P. G. Conformations of Polymers Attached to an Interface. *Macromolecules* **1980,** *13*, 1069-1075.

(44) Hamilton, W. A.; Smith, G. S.; Alcantar, N. A.; Majewski, J.; Toomey, R. G.; Kuhl, T. L. Determining the Density Profile of Confined Polymer Brushes with Neutron Reflectivity. *J. Polym. Sci. B: Polym. Phys.* **2004,** *42*, 3290-3301.

(45) Sirchabesan, M.; Giasson, S. Mesoscale Simulations of the Behavior of Charged Polymer Brushes under Normal Compression and Lateral Shear Forces. *Langmuir* **2007,** *23*, 9713-9721.

(46) Zangi, R.; Rice, S. A. Phase Transitions in a Quasi-Two-Dimensional System. *Phys. Rev. E* **1998,** *58*, 7529-7544.

(47) Kaganer, V. M.; Möhwald, H.; Dutta, P. Structure and Phase Transitions in Langmuir Monolayers. *Rev. Mod. Phys.* **1999,** *71*, 779-819.

(48) Zangi, R.; Rice, S. A. Nature of the Transition from Two- to Three-Dimensional Ordering in a Confined Colloidal Suspension. *Phys. Rev. E* **2000,** *61*, 660-670.

(49) Zangi, R.; Rice, S. A. Hexagonal to Square Lattice Conversion in Bilayer Systems. *Phys. Rev. E* **2000,** *61*, 671-681.

(50) Zhu, J.; Eisenberg, A.; Lennox, R. B. Interfacial Behavior of Block Polyelectrolytes. 6. Properties of Surface Micelles as a Function of R and X in P(S260-b-VP240/RX). *Macromolecules* **1992,** *25*, 6556-6562.

(51) Cox, J. K.; Lennox, R. B. Compression of Polystyrene–Poly(ethylene oxide) Surface Aggregates at the Air/Water Interface. *Phys. Chem. Chem. Phys.* **1999,** *1*, 4417-4421.

(52) Baker, S. M.; Leach, K. A.; Devereaux, C. E.; Gragson, D. E. Controlled Patterning of Diblock Copolymers by Monolayer Langmuir−Blodgett Deposition. *Macromolecules* **2000,** *33*, 5432-5436.

(53) Glagola, C. P.; Miceli, L. M.; Milchak, M. A.; Halle, E. H.; Logan, J. L. Polystyrene–Poly(ethylene oxide) Diblock Copolymer: The Effect of Polystyrene and Spreading Concentration at the Air/Water Interface. *Langmuir* **2012,** *28*, 5048-5058.

(54) Gonçalves da Silva, A. M.; Filipe, E. J. M.; d'Oliveira, J. M. R.; Martinho, J. M. G. Interfacial Behavior of Poly(styrene)−Poly(ethylene oxide) Diblock Copolymer Monolayers at the Air−Water Interface. Hydrophilic Block Chain Length and Temperature Influence. *Langmuir* **1996,** *12*, 6547-6553.

(55) Li, S.; Hanley, S.; Khan, I.; Varshney, S. K.; Eisenberg, A.; Lennox, R. B. Surface Micelle Formation at the Air/Water Interface from Nonionic Diblock Copolymers. *Langmuir* **1993,** *9*, 2243-2246.

(56) Cheyne, R. B.; Moffitt, M. G. Self-assembly of polystyrene-block-poly(ethylene oxide) copolymers at the air-water interface: is dewetting the genesis of surface aggregate formation? *Langmuir* **2006,** *22*, 8387-96.

(57) Shuler, R. L.; Zisman, W. A. Study of the Behavior of Polyoxyethylene at the Air-Water Interface by Wave Damping and Other Methods. *J. Phys. Chem.* **1970,** *74*, 1523-1534.

(58) Seo, Y.; Paeng, K.; Park, S. Molecular Weight Effect on the Behaviors of Polystyrene-block-poly(methyl methacrylate) Diblock Copolymers at Air/Water Interface. *Macromolecules* **2001,** *34*, 8735-8744.

(59) Xu, H.; Erhardt, R.; Abetz, V.; Müller, A. H. E.; Goedel, W. A. Janus Micelles at the Air/Water Interface. *Langmuir* **2001,** *17*, 6787-6793.

(60) Liou, J.-Y.; Sun, Y.-S. Monolayers of Diblock Copolymer Micelles by Spin-Coating from o-Xylene on SiOx/Si Studied in Real and Reciprocal Space. *Macromolecules* **2012,** *45*, 1963-1971.

For Table of Contents Only